REPORT DOCUMENTATION PAGE

Form Approved
OMB No. 0704-0188

1. REPORT DATE *(DD-MM-YYYY)*	2. REPORT TYPE	3. DATES COVERED *(From - To)*
27-01-2010	Final	21-03-2006 - 30-4-09

4. TITLE AND SUBTITLE
Turbulent drag reduction using micro and nanotextured ultrahydrophobic surfaces

5a. CONTRACT NUMBER
N/A

5b. GRANT NUMBER
N00014-06-1-0497

5c. PROGRAM ELEMENT NUMBER
N/A

6. AUTHOR(S)
Jonathan P. Rothstein

5d. PROJECT NUMBER
N/A

5e. TASK NUMBER
N/A

5f. WORK UNIT NUMBER
NA

7. PERFORMING ORGANIZATION NAME(S) AND ADDRESS(ES)
University of Massachusetts
70 Butterfield Terrace
Amherst, MA 01003-9333

8. PERFORMING ORGANIZATION REPORT NUMBER
N/A

9. SPONSORING/MONITORING AGENCY NAME(S) AND ADDRESS(ES)
Office of Naval Research
875 North Randolph St., Suite 1425
Arlington, VA 22203-1995

10. SPONSOR/MONITOR'S ACRONYM(S)
N/A

11. SPONSOR/MONITOR'S REPORT NUMBER(S)
N/A

12. DISTRIBUTION/AVAILABILITY STATEMENT
Approved for public release; distribution is unlimited.

13. SUPPLEMENTARY NOTES
N/A

20100201221

14. ABSTRACT
This final report documents the findings of our research project which demonstrated through a combination of experimental measurements and numerical simulations that ultrahydrophobic surfaces can be used to delay the transition to turbulence and dramatically reduce drag in both external and internal turbulent flows. These enhancements should have a profound effect on a huge variety of existing technologies, resulting in benefits ranging from a reduction in the pressure drop in pipe flows to an increase in speed and efficiency in surface ships and and small submersible vehicles.

15. SUBJECT TERMS
N/A

16. SECURITY CLASSIFICATION OF:			17. LIMITATION OF ABSTRACT	18. NUMBER OF PAGES	19a. NAME OF RESPONSIBLE PERSON
a. REPORT	b. ABSTRACT	c. THIS PAGE			Jonathan P. Rothstein
U	U	U	UU	16	19b. TELEPHONE NUMBER *(Include area code)* 413-577-0110

Final Report: N00014-06-1-0497
Name: Jonathan Rothstein
Organization: UNIVERSITY OF MASSACHUSETTS-AMHERST
City/State/Country: Amherst/MA/USA
Title: Assoc. Professor
Zip Code: 01003
Phone: 413-577-0110
Fax: 413-545-1024
Email: rothstein@ecs.umass.edu
Website: http://www.ecs.umass.edu/mie/faculty/rothstein/
Contract Information
Contract/Grant Number: N00014-06-1-0497
Contract/Grant Title: Turbulent drag reduction using micro and nanotextured ultrahydrophobic surfaces
Program Officer: Ron Joslin
Abstract
The main objective of this research project is to demonstrate through a combination of experimental measurements and numerical simulations that ultrahydrophobic surfaces can be used to delay the transition to turbulence and dramatically reduce drag in both external and internal turbulent flows. These enhancements could have a profound effect on a huge variety of existing technologies, resulting in benefits ranging from a reduction in the pressure drop in pipe flows, to improved microfluidic devices, to an increase in range of small submersible vehicles. In short, almost any device that uses or interacts with liquids has the potential to benefit from the ultrahydrophobic surface technologies that will be developed through the research performed for this contract.
Technical Section
See pages 4-16
Final Progress Statement
Over the past year we have been investigating the turbulent drag reduction properties of ultrahydrophobic surfaces through both detailed experiments and direct numerical simulations. Our results demonstrate drag reduction of up to 75% using ultrahydrophobic surfaces with slip lengths of over 120 microns. The drag reduction is observed to begin after the flow has become fully turbulent at or near Re = 4000 and to increase with increasing Reynolds number and microfeature spacings. The simulation results were recently published in the Journal of Fluid Mechanics with a second paper submitted to Physics of Fluids. Our experimental results were recently published in Physics of Fluids and my recent Annual Review of Fluid Mechanics article.
Technology Transfer
In May of 2009 we applied for a provisional patent based on our ONR funded research. The patent is entitled "Design of Superhydrophobic Surfaces for Drag Reduction." We hope to license and commercialize this technology in the coming year.
Refereed Journal Articles
1. Martell, M. B., Perot, J. B., and Rothstein, J. P., "Direct numerical simulations of turbulent flows over superhydrophobic surfaces," J. Fluid Mech., 620 (2009) 31-41.
2. Daniello, R., Waterhouse, N. E., and Rothstein, J. P., "Turbulent drag reduction using superhydrophobic surfaces," In Press in Phys. Fluids, (2009).
3. Martell, M. B., Rothstein, J. P., and Perot, J. B., "The effect of Reynolds number on turbulent flows over superhydrophobic surfaces," Submitted to Phys. Fluids, (2009).
4. Daniello, R., Gabour, J., and Rothstein, J. P., "The effect of superhydrophobic surface geometry on turbulent drag reduction," Submitted to J. Fluid Mech., (2009).

5. Rothstein, J. P., "Slip on Superhydrophobic Surfaces," in press in Annu. Rev. Fluid Mech., 42 (2010).
6. Nilsson, M., Daniello, R., and Rothstein, J. P., "A novel and inexpensive technique for creating superhydrophobic surfaces using Teflon and sandpaper," to be submitted to Nature Materials, (2009).

Books and Chapters

1. Rothstein, J. P., "Strong Flows Of Viscoelastic Wormlike Micelle Solutions," in Binding, D. M., and Walters, K., eds., Rheology Reviews, The British Society of Rheology, Aberystwyth, Wales, UK, 2008.

Technical Reports

None entered

Contributed Presentations

1. J.P. Rothstein. "Drag Reduction in Laminar and Turbulent Flows Past Superhydrophobic Surfaces," Invited talk at UCLA, May 2009.
2. M. Martell, Blair Perot, and J.P. Rothstein, "DNS of Turbulent Channel Flow past Ultrahydrophobic Surfaces with Periodic Microfeatures" Presented at APS Division of Fluid Dynamics Annual Meeting, San Antonio, TX, November 2008.
3. R. Daniello and J.P. Rothstein, "Experimental Measurements of Turbulent Drag Reduction Using Ultrahydrophobic Surfaces with Periodic Microfeatures" Presented at APS Division of Fluid Dynamics Annual Meeting, San Antonio, TX, November 2008.

Patents

1. R. Daniello and J.P. Rothstein, "Design of Superhydrophobic Surfaces for Drag Reduction," provisional patent submitted 2009

Honors

1. Arthur B. Metzner Early Career Award to Jonathan Rothstein of University of Massachusetts from the Society of Rheology. This award was presented in recognition of outstanding accomplishments in the field of rheology.

Related Sponsored Work

None entered

ONR Statistics

Papers Published: 6
Papers In Press: 0
Books/Chapters: 1
Books/Chapters In Press: 0
Technical Reports: 0
Invention Disclosures: 0
Patents Awarded: 1
Patents Pending: 0
Presentations: 0
Contributed Presentations: 3
Degrees Granted: 2
Honors: 1
Co-PIs: 0
Women Co-PIs: 0
Minority Co-PIs: 0
Graduate Students (Total): 2
Women Graduate Students: 0
Minority Graduate Students: 0
Undergraduate Students (Total): 1
Women Undergraduate Students: 0
Minority Undergraduate Students: 0

Post Doctoral Students (Total): 0
Women Post Doctoral Students: 0
Minority Post Doctoral Students: 0

Contract Information

Contract Number	N00014-06-1-0497
Title of Research	Turbulent Drag Reduction Using Micro and Nanotextured Ultrahydrophobic Surfaces
Principal Investigator	Jonathan P. Rothstein
Organization	University of Massachusetts.

Technical Section

Technical Objectives

The interaction between solid surfaces and liquids is of fundamental importance in engineering flows where solid surfaces are the primary means for controlling or manipulating fluids. We will show that by treating a solid surface to make it ultrahydrophobic it is possible to significantly enhance how the surface interacts with a flowing liquid. In particular, in our recent work, we have shown that ultrahydrophobic surfaces can be utilized to reduce drag [2, 3] and enhance mixing [4] in low to moderate Reynolds number internal flows. The main objective of this research project is to demonstrate through a combination of experimental measurements and numerical simulations that ultrahydrophobic surfaces can also be used to delay the transition to turbulence and dramatically reduce drag in both external and internal turbulent flows. These enhancements could have a profound effect on a huge variety of existing technologies, resulting in benefits ranging from a reduction in the pressure drop in pipe flows, to improved microfluidic devices, to an increase in range of small submersible vehicles. In short, almost any device that uses or interacts with liquids has the potential to benefit from the ultrahydrophobic surface technologies that will be developed through the research proposed here.

The presence of drag reduction using ultrahydrophobic surfaces had been suggested previously by a number of other authors [5-7]. However, prior to our experiments and numerical simulations [2-4], the results of other researchers were somewhat ambiguous and a number of different theories were presented to explain the observed drag reduction. In our previous work, a detailed experimental study was performed which unequivocally demonstrated the existence of drag reduction in laminar flows with ultrahydrophobic surfaces. Ultrahydrophobic surfaces are engineered by taking materials with micron or nanoscale surfaces roughness and chemically treating them to make them hydrophobic. When water is brought in contact with an ultrahydrophobic surface, the water is completely supported by the peaks in the surface topology as seen in Figure 1. Because of the hydrophobicity of these microscale and nanoscale protrusions, the water does not move into the pores on the surface, rather it remains in contact with only the peaks of the surface topology resulting in a shear-free air-water interface. The underlying physical mechanism for drag reduction is a slip along the shear-free air-water interface supported between the peaks of micro or nanoscale protrusions present on the ultrahydrophobic

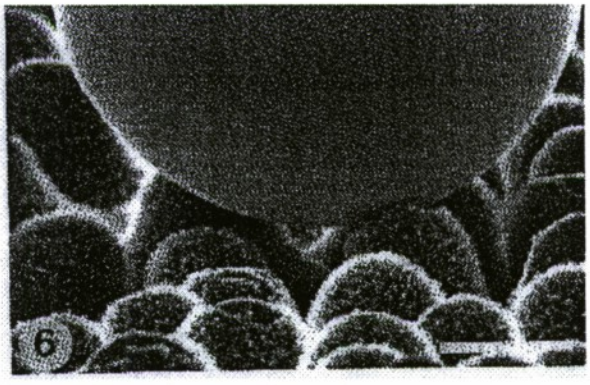

Figure 1. Micrographs of a water droplet in contact with an ultrahydrophobic lotus leaf. The droplet is supported by the hydrophobic micro-posts populating the surface of the lotus leaf. (from [1]) .

surface. This physical mechanism was validated for laminar flows through direct observation of the interface using laser confocal metrology, direct velocity measurement using micro particle image velocimetry (μ-PIV), and direct comparison to numerical simulations and analytical theory [2-4]. One of the major objectives of this project is to demonstrate that these same surfaces can also reduce drag when the flow is turbulent.

Once we have fully understanding the physical mechanism of ultrahydrophobic drag reduction our goal will be to configure the microscopic features of the surface to optimize its performance under different design criteria. We originally used etched silicon wafers in order to precisely control the micro-geometry and therefore unambiguously control the micro-characteristics of and flow characteristics near the ultrahydrophobic surface, but we have recently been able extend our technique to more flexible materials like polydimethylsiloxane (PDMS) through soft lithography and pressed Teflon. The use of these well-designed surfaces has and will enable us to perform exactly matching computational fluid dynamics of the flow near these ultrahydrophobic surfaces [3, 4].

In summary, the technical objectives of this research project are to: (1) demonstrate that turbulent drag reduction is possible with these surfaces; (2) confirm that the transition to turbulence is delayed; and finally to (3) develop techniques for fabricating large area sheets of ultrahydrophobic surfaces with nanometer length features for use in deep-sea applications. The goal is to understand precisely how these materials behave, maximize their efficiency and determine under what circumstances they are the most useful.

Technical Approach

Experiments

An experimental flow cell was fabricated for taking pressure drop and particle image velocimetry (PIV) measurement of the turbulent flow past ultrahydrophobic surfaces. An image of the flow cell is shown in Figure 2. In the flow cell the top wall is always smooth and optically clear for PIV and the bottom wall is changeable and could be smooth or ultrahydrophobic. The flow cell is 2in wide, 3ft long and has a height that is variable from 1/8in to 1/2in high. A gravity feed system is used to isolate the flow from the vibrations and fluctuations of the pump which is capable of driving flows up to a Reynolds number of approximately $Re = UH/\nu = 10{,}000$. Here U is the average velocity in the channel, H is the height of the channel and ν is the viscosity of the fluid. A flow meter is used to determine the flow rate and average Reynolds number in the channel and a series of differential pressure transducers are used to measure the pressure drop. Additionally, a PIV system is installed using an Argon Ion laser and a high-speed video camera to take instantaneous and time averaged measurements of the velocity and turbulent statistics within the flow. The images are processed using the commercial PIV software LaVision.

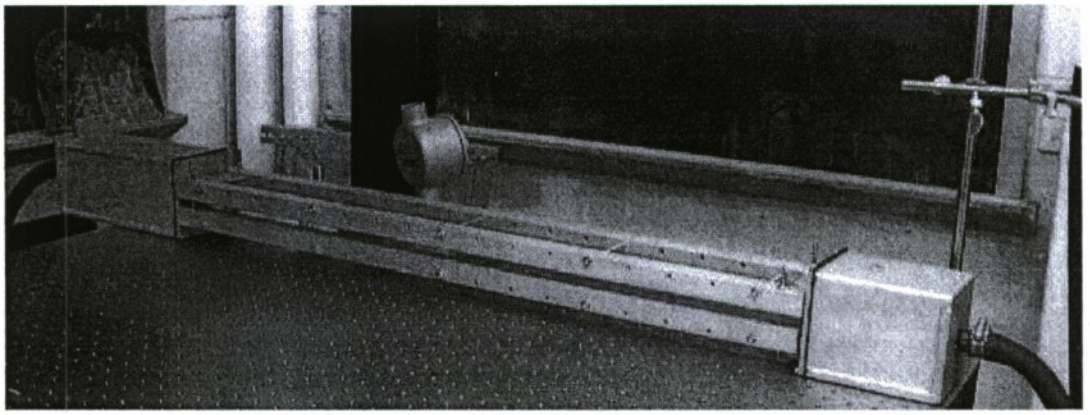

Figure 2. Experimental flow cell used for ultrahydrophobic drag reduction measurements.

Ultrahydrophobic surfaces created by using either standard photolithographic techniques to etch silicon wafers [2, 8] or soft lithography to produce precise micropatterns in PDMS [9] or through a new technique we have developed to cold-work metal mesh screens into Teflon. A schematic diagram outlining the fabrication procedure for lithographically etched ultrahydrophobic surfaces is shown in Figure 3. First, a CAD package is used to design the size, spacing and alignment of the desired micro-patterned surface. The file is then printed on a high-resolution transparency at 5080 dpi. The transparency serves as a mask for contact photolithography using a positive photoresist on a silicon wafer [10]. At this point there are two options; to use either wet or DRIE etching techniques to create the desired pattern in the silcon surface as shown in Figure 3 or to use a photoresist like SU-8 which can create robust features without the need for etching that can be up to 100μm tall. The silicon wafer is in turn used as a master for creating a negative of its pattern in PDMS using soft lithography [9]. The PDMS surface is then cleaned using a plasma etcher and silanized under a vapor reaction with an organosilane reagent [11]. These ultrahydrophobic surfaces can have advancing contact angles as large as θ=165°. Soft lithography is non-photolithographic technique developed for rapidly replicating a micropattern. The micropatterns of interest are transferred to the PDMS through replica molding from a master creating a negative replica in the PDMS. The master can be a photolithographically etched silicon wafer or any other surface with the desired surface roughness. After being spun onto or compressed into the surface of the master, the PDMS is cured in an oven and the replica is peeled from the master creating a micropatterned surface on a flexible elastomer substrate. It is naturally hydrophobic without further chemical reaction and it can be applied to almost any substrate or scaffold while maintaining the ordered and precise patterning that makes the use of silicon wafers so desirable.

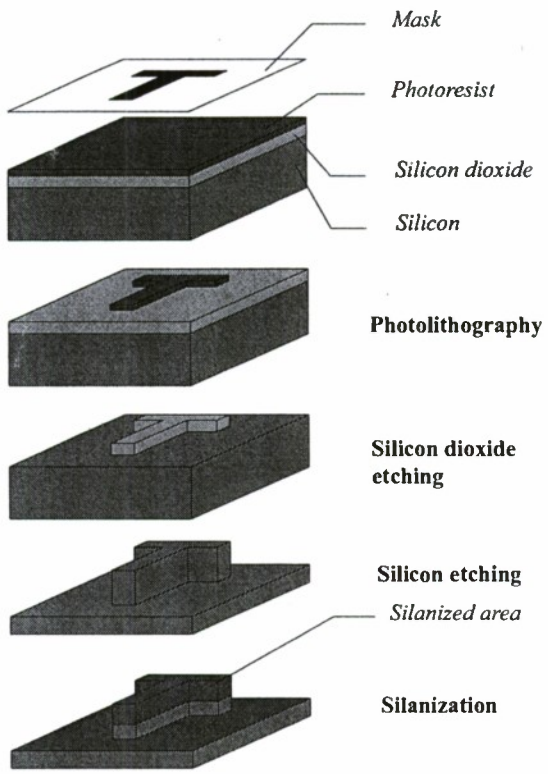

Figure 3. Schematic diagram of the method used for creation of ultrahydrophobic surfaces.

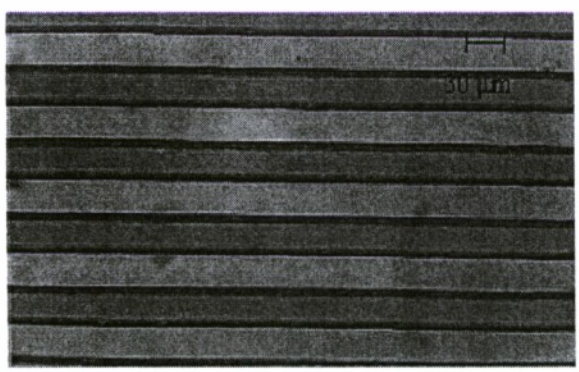

Figure 4. Example of an ultrahydrophobic surface made from PDMS with 30μm wide microridges spaced 30μm apart

To fabricate a very large ultrahydrophobic surface, a number of 6in PDMS surfaces were patched together using fast curing PDMS as glue. Great care was taken to minimize the profile of the seams. The quality of the patches were confirmed with surface profilometry measurements. We are also working on a number of techniques to produce long seemless ultrahydrophobic surfaces. We are currently developing a roll-to-roll system capable of transferring precise

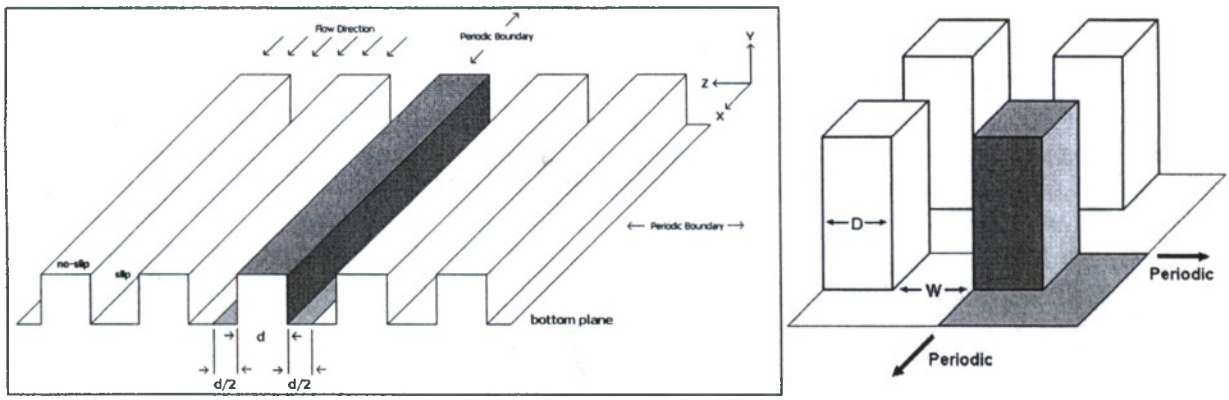

Figure 5. Schematic diagram of an ultrahydrohobic microridge currently being modeled. Note that the ridge height does not exist in code. The 'top' of the ridges have a no-slip boundary condition, and the 'space' between the ridges have a slip boundary condition.

patterns onto a film in a continuous and seamless fashion.

Experiments have been performed with a range of different surfaces. For the purpose of this progress report we will focus on the results from two surfaces: a 30μm wide microridges spaced 30μm apart as seen in Figure 4 and a 60μm wide microridges spaced 60μm apart for which we have the most data, but will also discuss surfaces with other geometries as well.

Numerical Simulations

Direct numerical simulations are currently being performed for flow over a series of model ultrahydrophobic surfaces chosen to directly match the surfaces used in the experiments. In the simulations, the top of the microposts or microridges are assumed to be no-slip and the air-water interface between them is assumed to be shear-free and flat. Both of these assumptions are reasonable, however, under certain conditions, the air-water interface can deflect and the recirculation of air within the gaps between the microposts or microridges can produce some drag along the air-water interface. Quantifying the contribution of both of these effects is important and is planned for the final year of this project. The simulation domain currently contains ten or more microridges and periodic boundary conditions on the side walls as seen in Figure 5. The numerical algorithm used to simulate the has been under development for almost a decade [12, 13] and over the last year it has been modified to apply directly to turbulent flows past ultrahydrophobic surfaces. The code uses non-uniform grid spacing to place more resolution near the channel walls and a Cartesian staggered mesh method [14] with exact projection [15] for the pressure solution. The Navier-Stokes equations are solved using a conjugate gradient solver and a modified Runge-Kutta time marching method [16]. The code is fully parallelized [17] (with MPI) for PC cluster architectures. The code is currently running on the Navy's supercomputer sight in Alaska with resolutions of 128^3, 256^3 and 512^3.

Progress Statement Summary

Over the course of the past year we have been investigating the turbulent drag reduction properties of ultrahydrophobic surfaces through both detailed experiments and direct numerical simulations. On the experimental side, we have fabricated a flow cell and developed a number of techniques for producing large-scale surfaces containing precise micron-scale patterns of microridges and microposts. Using both pressure drop measurements and particle image velocimetry measurements our results demonstrate drag reduction of up to 75% using ultrahydrophobic surfaces with slip lengths of over 120μm. The drag

reduction is observed to begin after the flow has become fully turbulent at or near Re = 4000 and to increase with increasing Reynolds number to the limit of our experiments at Re = 10,000. On the numerical simulation side, we modified an existing direct numerical simulation code to perform simulations with walls having periodic slip no-slip boundary conditions to simulate the flow over hydrophobic microridges and microposts. The code is now fully operational and parallelized having been benchmarked against simulation results in the open literature for flow within rectangular channel with smooth walls at 128^3, 256^3 and 512^3. We have simulating turbulent flow over ultrahydrophobic surfaces containing both microridges and microposts that match and extend those used in the experiments. The simulations agree quite well with the experimental results and demonstrate drag reductions and slip velocities which increase with increasing spacing between microfeatures and Reynolds number. The DNS work for 128^3 simulations was recently published in the Journal of Fluid Mechanics [18] as a fast track article and a follow up article with results for higher Reynolds numbers was recently submitted to Physics of Fluids [19]. Our experimental results were recently accepted as a featured article in Physics of Fluids [20] and a second paper with the results from a number of different surface geometries is currently being prepared for submission to Journal of Fluid Mechanics [21]. This work has been presented at a number of national and international conferences and workshops and has been featured in my recent Annual Review of Fluid Mechanics article [22] entitled "Slip on Superhydrophobic Surfaces."

Progress

Experiments

To date we have concentrated our efforts on taking measurements of the flow past a smooth PDMS surface and a series of ultrahydrophobic surfaces consisting of 10μm, 15μm, 30μm and 60μm wide microridges spaced between 15μm and 60μm apart. For sake of brevity, in this progress report, we will focus primarily on two geometries a 30μm wide microridges spaced 30μm apart as seen in Figure 4 and a 60μm wide microridges spaced 60μm apart, but we will also present highlights from the best surfaces studied to date.

A typical set of velocity profiles, resulting from PIV near the superhydrophobic wall for the 60-60 ridge surface is shown in Figure 6a for a range of Reynolds number between 2700< Re < 8200. The effect of the superhydrophobic wall is not observed for the low Reynolds number experiments. At the low Reynolds numbers, the turbulent velocity profiles just past transition are, to the limit of our measurements, equivalent to smooth profiles at identical Reynolds numbers This is not unexpected for the data points in the laminar or transitional regime [2, 3]. In laminar flows, superhydrophobic surfaces of similar size and geometry demonstrated slip lengths which were independent of flow rate and approximately b = 25μm [3]. For pressure driven flow between two infinite parallel plates separated by a distance 2δ the volume flow rate per unit depth is given by

$$q = \frac{2\delta^3}{\mu}\left(-\frac{dp}{dx}\right)\left[\frac{1}{3}+\frac{b}{b+2\delta}\right]. \qquad (1)$$

For a given pressure gradient, dp/dx, and fluid viscosity, μ, the volume flow rate can be significantly enhanced only if the slip length is comparable to the channel height. Previous laminar regime studies over similar superhydrophobic microfeatures measured slip lengths of b = 25μm independent of Reynolds number [2]. In our channel geometry, such laminar flow slip lengths would produce a drag reduction of around 1%. Additionally, for small slip lengths, the expected slip velocity can be approximated by $u_{slip} = 4Ub/\delta$ which should also be on the order of only a couple of percent of the average free stream velocity, U, and below the resolution of our PIV measurements. As the Reynolds number is increased and the flow becomes fully turbulent, however, a substantial slip velocity, and slip lengths greater than b = 25μm, are observed along the superhydrophobic wall. The presence of an air

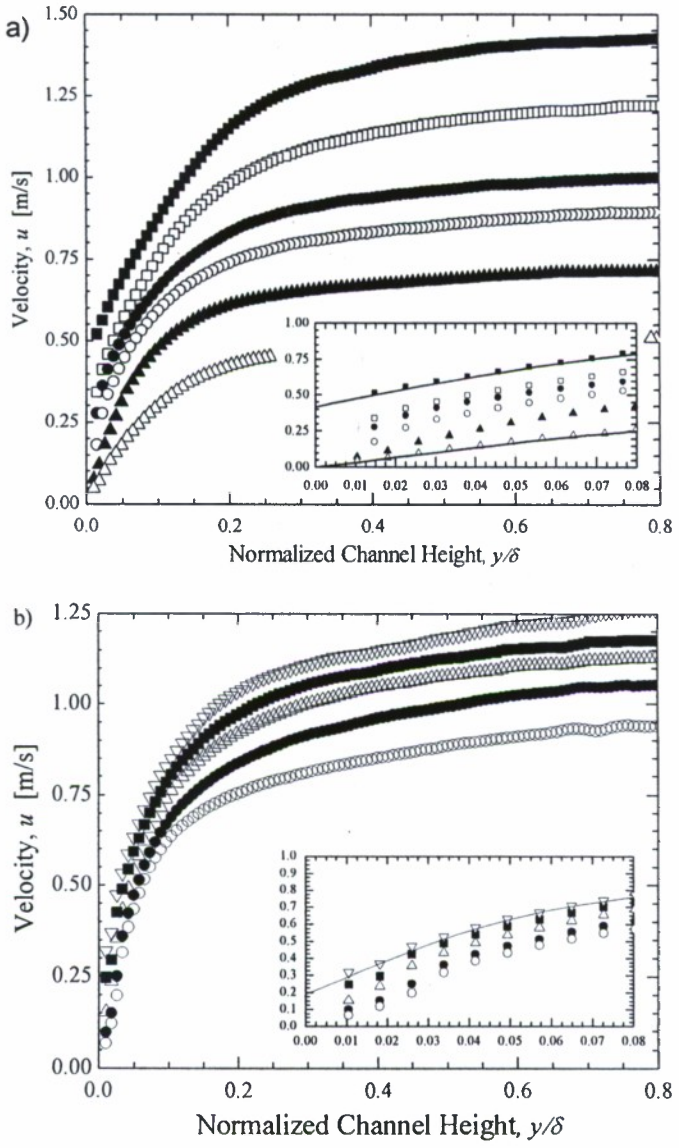

Figure 6. a.) Velocity profiles over a microridge surface w = 60μm d = 60μm showing the development of significant slip velocities with increasing Reynolds number from 2700 (Δ) to 8200 (■). (Inset) Velocity profiles near the wall demonstrating prominent slip velocities. Reynolds numbers are: 2700 (Δ), 3900 (▲), 4840 (◊), 5150 (♦), 6960 (□), 8200 (■). For clarity, the modified Spalding fits (—) from Equation 3 are only overlaid on the profiles corresponding to Re=2700 and Re=8200. b.) Velocity profiles over the w = 30μm d = 30μm microridge surface demonstrate slip velocity behavior consistent with that observed on the 60-60 surface, but reduced in magnitude. Reynolds numbers range from 4970 (○) to 7930 (▽). Larger feature spacing performs better for a given Reynolds number. Reynolds numbers are: 4970 (○), 5400 (♦), 6800 (Δ), 7160 (■), 7930 (▽) The modified Spalding fits (—) are overlaid on the profile corresponding to Re=7930.

water interface is visually apparent on the superhydrophobic surface giving it a silvery appearance. This result, due to the differing indices of refraction and slight curvature of the interface, was observed throughout the range of testing giving us confidence that the interface was maintained for all of the experiments reported in this paper.

As the inset of Figure 6a clearly shows, the magnitude of the slip velocity was found to increase with increasing Reynolds number. Similar, although less pronounced, trends were observed for the 30-30 ridge case as seen in Figure 6b. Significant deviation from no-slip behavior is noted past a Reynolds number of approximately Re = 4000 for both the 30-30 and 60-60 ridged cases. Above these Reynolds numbers, a nearly linear increase in the slip velocity with increasing Reynolds number was observed for each of the superhydrophobic surfaces used. A maximum slip velocity of nearly 40% the mean channel velocity, $u_{slip}/U = 0.4$ was observed for the 60-60 ridged case at the highest Reynolds numbers tested.

In order to determine both the shear stress and slip velocity at the smooth and superhydrophobic walls, the PIV velocity fields were fit to a modified Spalding equation for turbulent velocity profile above a flat plate [23],

$$y^+ = \left(u^+ - u^+_{slip}\right) + e^{-2.05}\left[e^{-0.41\left(u^+ - u^+_{slip}\right)} - 1 - 0.41\left(u^+ - u^+_{slip}\right) - \frac{1}{2}\left(0.41\left(u^+ - u^+_{slip}\right)\right)^2 - \frac{1}{6}\left(0.41\left(u^+ - u^+_{slip}\right)\right)^3\right] \quad (2)$$

The Spalding equation is an empirical fit to experimental turbulent velocity profile data that covers the entire wall region through the log layer [24]. This allows the fit to be applied farther into the channel, to determine the wall shear stress more accurately using a greater number of data points than would be available within the viscous sublayer. Wall shear stress enters the equation in the definition of the velocity, u^+, and position y^+, in wall units. To account for slip, each instance of the velocity in wall units, $u^+ = u\sqrt{\rho/\tau_w}$, in the Spalding equation was replaced by the difference $u^+ - u^+_{slip}$. The fit was performed by a numerical routine given an initial value for slip velocity extrapolated from a coarse linear fit of near wall data points. An initial wall shear stress was determined by minimizing the error in the fit. Subsequent iterations were performed on wall slip velocity and wall shear stress to minimize the standard error of the fit over the interval $0 < y^+ < 50$. The resulting fits were accurate to better than 4% at a 95% confidence interval. The results were not appreciably different if the fit is taken to $y^+ = 100$. The size of the PIV correlation window was chosen to be 0.2mm. For the frame rates used, the resulting particle displacements within the correlation window were typically much less than 25% of the window in the viscous sublayer and less than 33% of the window everywhere for Reynolds numbers less than Re < 4500. Large particle displacements were observed far from the wall at the highest Reynolds numbers, however, no noticeable effects were observed on the resulting profiles.

As seen in Figure 6, the resulting fits of Equation 3 to the velocity profiles are excellent with and without slip, which instills confidence in the values of shear stress calculated from the velocity gradient extrapolated to the wall, $\tau_w = \mu\left(\partial u/\partial y\right)\big|_{y=0}$. The maximum slip velocity and observed wall shear stress reductions correspond to slip lengths of $b > 70\mu m$ for the 30-30 microridges and $b > 120\mu m$ for the 60-60 microridges. Larger slip velocities and slip lengths were measured for turbulent flow past superhydrophobic surfaces with larger microfeature spacings even as the percentage of shear-free interface was kept constant at $w/(w+d)$ = 0.5, as has been observed in the laminar flow measurements over superhydrophobic surfaces [3]. This observation is consistent previous laminar flow studies[2, 3] and with the predictions of DNS in turbulent flows [25]. Additionally, Ybert *et al.* [26] showed through a scaling argument that in laminar flows one expects the slip length to scale linearly with the microfeature spacing, $b \propto (w+d)$.

In Figure 7, direct measurements of the pressure drop per unit length of channel, dp/l, are shown for a smooth PDMS surface and the superhydrophobic surface containing 60μm ridges spaced 60μm apart and a surface containing 10μm ridges spaced 60μm apart in an identical channel. The result predicted by the Colebrook equation [27] for a perfectly smooth channel of the same dimension is plotted

for reference. The pressure drop per unit length is directly related to the channel geometry and the wall shear stress, $dp/l = \tau_w\left(1+2\delta/W\right)/\delta$, so it provides a second method for measuring drag reduction. Significant drag reduction is initially noted by a leveling off of the in the pressure drop during the transition from laminar to turbulent flow between Reynolds numbers of 2000 < *Re* < 3000. These data indicate a delay in the transition to fully-developed turbulent flow and an increased drag reduction with increased microridge spacing. Additionally, for Reynolds numbers greater than *Re* > 3000 the pressure drop over the 60-60 surperhydrophobic surface grows at roughly half the rate of pressure drop over the smooth surface while the 60-10 grows at less than one quarter the rate of the smooth surface. The Colebrook line, accurately fits the turbulent flow data from the smooth surface, and the predicted laminar flow result passes through the microridge data in the laminar region below *Re* < 2200. This result is consistent with those predicted by Equation 2 and observed by PIV. As noted before there is no measurable drag reduction or slip velocity for the present channel geometry in the laminar regime.

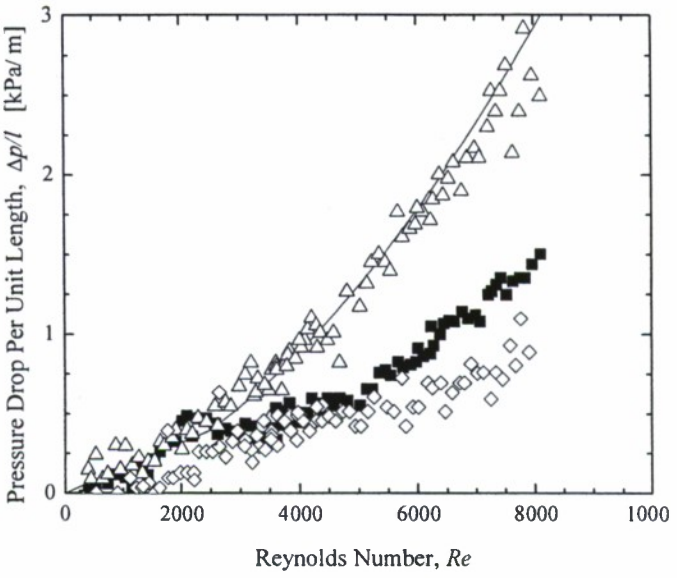

Figure 7. Pressure drop measurements for flow through a rectangular channel with a smooth walls (Δ) and with two walls containing superhydrophobic microridges with *w*=60μm and *d*=60μm (■) and *w*=60μm and *d*=10μm (◊). The Colebrook line (—) is shown for a smooth channel.

In Figure 8, the wall shear stresses, τ_w, calculated from the Spalding fit to the velocity profiles and from pressure measurements of smooth, 30-30 and 60-60 channels are non-dimensionalized to form a coefficient of friction, $C_f = 2\tau_{wall}/\rho U^2$, and plotted as a function of Reynolds number. For comparison, the Colebrook prediction of friction coefficient for the present perfectly smooth channel is superimposed over the data in Figure 8. Friction coefficient was selected to account for small variations in channel height existing between the pressure drop and PIV experiments. As previously indicated, the friction coefficients of the smooth wall, calculated from PIV, and that of the smooth channel, determined from pressure drop, are in good agreement with each other as well as with the Colebrook prediction. At low Reynolds numbers, in the absence of any quantifiable slip at the superhydrophobic wall, the coefficient of friction for all cases tracks with that of the smooth-walled channel. At larger Reynolds numbers, where slip velocities are observed, the coefficients of friction of the superhydrophobic surfaces were found to lie well below those of the smooth channels. The drag reduction was found to increase with increasing Reynolds number and feature spacing, becoming more significant for *Re* > 5000 as observed in the pressure measurements. The 60-10 surfaces appear to fully relaminarize the flow resulting in nearly 75% drag reduction at high Reynolds numbers. The PIV measurements of the channel with a 30-30 superhydrophobic microridge surface on one wall and a smooth no-slip surface on the opposing wall show a somewhat smaller drag reduction than that which is noted by pressure drop along with two superhydrophobic walls. This result is likely due to differences in the flowcell geometry, specifically, the presence of the smooth wall in the PIV measurements, which was necessary to have transparency for flow visualization. The smooth wall has a higher wall shear stress than the superhydrophobic surface resulting in an asymmetric velocity profile and an increase in the turbulence intensity near the smooth wall. These observations were also made by Martell *et al.* [25] [28] for a DNS of channel flow with a single superhydrophobic wall. Observed drag reductions and slip velocities are in good agreement with

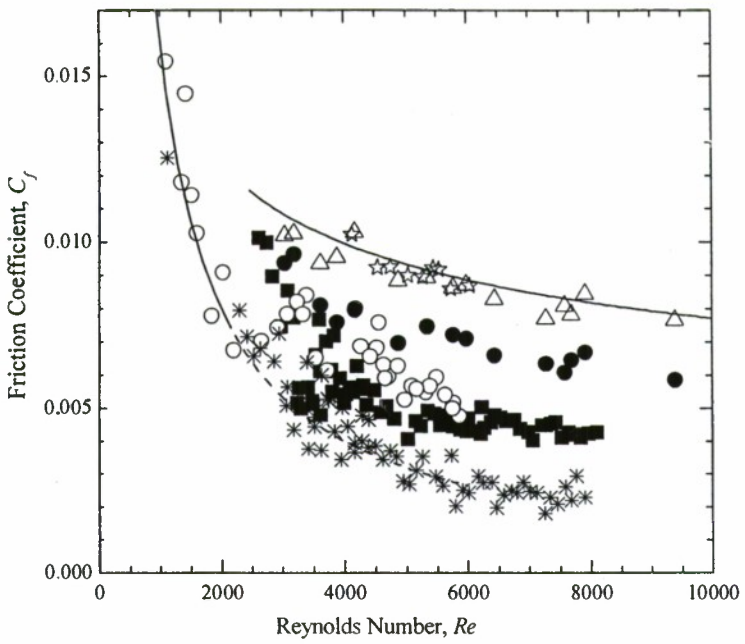

Figure 8. Coefficient of friction for various surfaces calculated from both PIV and pressure measurements. Smooth surfaces (Δ) and superhydrophobic surfaces containing w=30μm wide microridge spaced d=30μm apart (•) are shown for PIV measurements of a channel with a single superhydrophobic wall. Pressure drop measurements from channels with two smooth walls (☆) and two superhydrophobic walls containing w=30μm and d=30μm microridges (○), w=60μm d=60μm microridges (■) and w=60μm d=10μm microridges (*) are also shown. The predictions of the friction coefficient for a smooth channel is also shown (—) in both the laminar and turbulent regimes. Transition occurs around Re = 2100.

predictions for a DNS at $Re_\tau = 180$, corresponding to an experimental Re=5300 in the PIV data. DNS slightly over predicts slip velocity, and slightly under predicts drag reduction at 11% and reports enhanced performance with increasing microfeature size, as observed in the experiments. It should also be noted that DNS of Martell *et al* [25] [28] does not include interface deflection or compliance effects. Drag reduction calculated from PIV data are in excellent agreement with the slip length boundary condition DNS of Min and Kim [29] and predictions of Fukagata *et al.* [30] for streamwise slip. Both groups reported approximately 21% drag reduction [29, 30] at the same dimensionless slip length and friction Reynolds number observed in the present experiments at Re=5300. Given the challenges of directly matching DNS and experiments, these results are quite encouraging.

The turbulent drag reduction, $D_R = \left(\tau_{no-slip} - \tau_{SH}\right)/\tau_{no-slip}$, was computed as the percent difference in shear stress at the superhydrophobic and no-slip wall and is presented in Figure 9 as a function of Reynolds number. Drag reduction is presented rather than slip length because the slip length is difficult to quantify from the pressure drop measurements in turbulent flows. The slip length calculated from PIV data is insignificant in the laminar region and obtains a maximum value greater than b = 70μm for 30-30 and greater than b = 120μm for 60-60 ridges. In the present experiments, a maximum drag reduction of approximately 50% was observed for both microridge geometries once a suitably high Reynolds number was achieved. Drag reduction is initiated at a critical Reynolds number in the turbulent regime. For the microridges under present consideration, the critical Reynolds number was determined to be $Re_{crit} \approx 2500$. This Reynolds number is at or just past the transition to turbulent flow. This observation, along with the noted lack of drag reduction in the laminar regime, suggest that the underlying physical cause of the observed turbulent drag reduction must relate to the unique structure of wall-bounded turbulent flow.

The physical origins of the critical Reynolds number for the onset of drag reduction can be understood by analyzing the relevant lengthscales in the flow. If the drag reduction and the slip length were dependent on the microridge geometry and channel dimensions alone, as is the case in laminar flows, then we would expect to find the drag reduction and slip length to be independent of Reynolds number. In turbulent flows, however, there is a third lengthscale of importance, the thickness of the

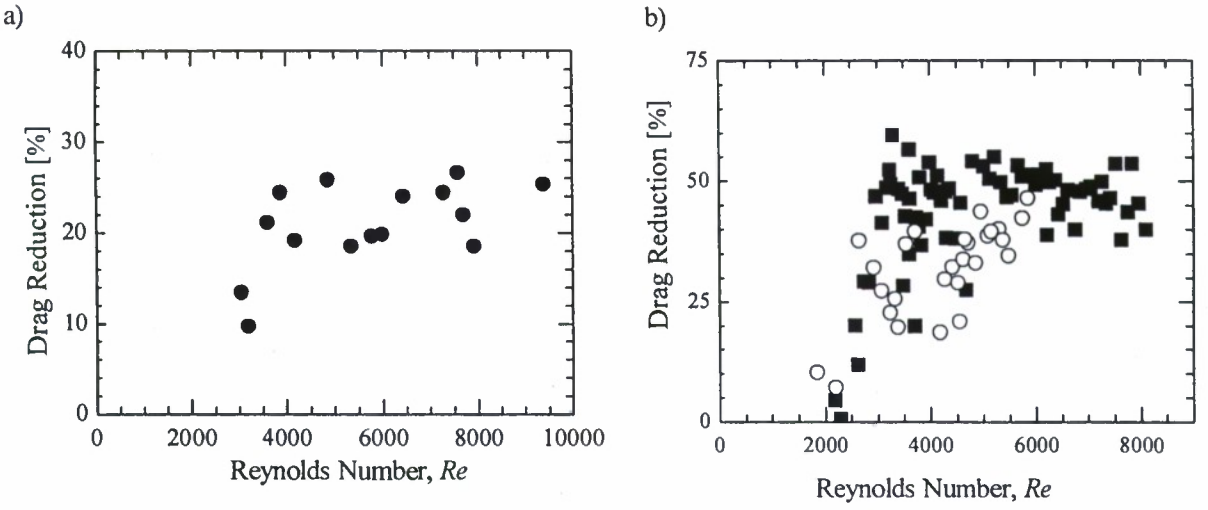

Figure 9. Drag reduction as a function of Reynolds number for a channel with a) a single superhydrophobic wall w=30μm d=30μm (●) and b) two superhydrophobic walls containing w=30μm and d=30μm microridges (○) and w=60μm and d=60μm microridges (■).

viscous sublayer which extends out to $y^+ = 5$. Although the viscous sublayer thickness remains fixed in wall units, in dimensional form the thickness of the viscous sublayer decreases with increasing Reynolds number as $y_{vsl} = 5\nu\sqrt{\rho/\tau_w}$. Close to the wall, where viscous stresses dominate, the analytical solutions of Philip [31, 32] show that the influence of the shear-free air-water interface extends to a distance roughly equal to the microridge spacing, w, into the flow. Thus for the superhydrophobic surface to impact the turbulent flow, the microridge spacing must approach the thickness of the viscous sublayer, $w \approx y_{vsl}$, or in other words $w^+ = y^+ \approx 5$. The microfeature spacing in wall units is at least $w^+ > 0.75$ for all the 30-30 surfaces tested and $w^+ > 2.4$ for the 60-60 surfaces. The w^+ values are calculated from shear stress measured at the superhydrophobic surface. This means that the microfeature spacing is minimally 15% to 50% of viscous sublayer thickness almost immediately after the turbulent transition. Hence for 30-30 and 60-60 ridges, drag reduction is noticed almost as soon as a turbulent flow develops. In laminar flows, significant drag reduction is noted at feature to height ratios comparable to those seen with the present feature size and viscous sublayer thickness [33]. A similar scaling has been observed for turbulent flow over wetted, rough surfaces, where the effects of roughness are not observed until the size of the roughness exceeds the thickness of the viscous sublayer [34]. As the Reynolds number increases and the thickness of the viscous sublayer is further reduced, the presence of the superhydrophobic surface will more strongly influence the velocity profile within the viscous sublayer and reduce the momentum transferred from the fluid to the wall and the vorticity of the fluid at the edge of the viscous sublayer. Turbulence intensity is thereby reduced, increasing the drag reduction. One therefore expects that saturation of the turbulent drag reduction is likely in the limit of very large Reynolds numbers where the microridges are much larger than the viscous sublayer. In this limit, the drag reduction should approach a limit of $D_R = w/(d+w)$ as momentum is only transferred from the solid fraction of the superhydrophobic surface and the viscous sublayer is thin enough that the no-slip and shear-free portions of the surface can be considered independently. For the present shear free area ratios, this limit would be 50%. This is consistent with both the asymptotic value of our PIV and pressure drop measurements. Drag reduction results shown in Figure 9 appear consistent with this hypothesis, the 60-60 ridges already appearing to plateau. As the critical Reynolds number will decrease with increasing feature spacing, coarser superhydrophobic surfaces will begin to perform better at lower Reynolds numbers. It is therefore

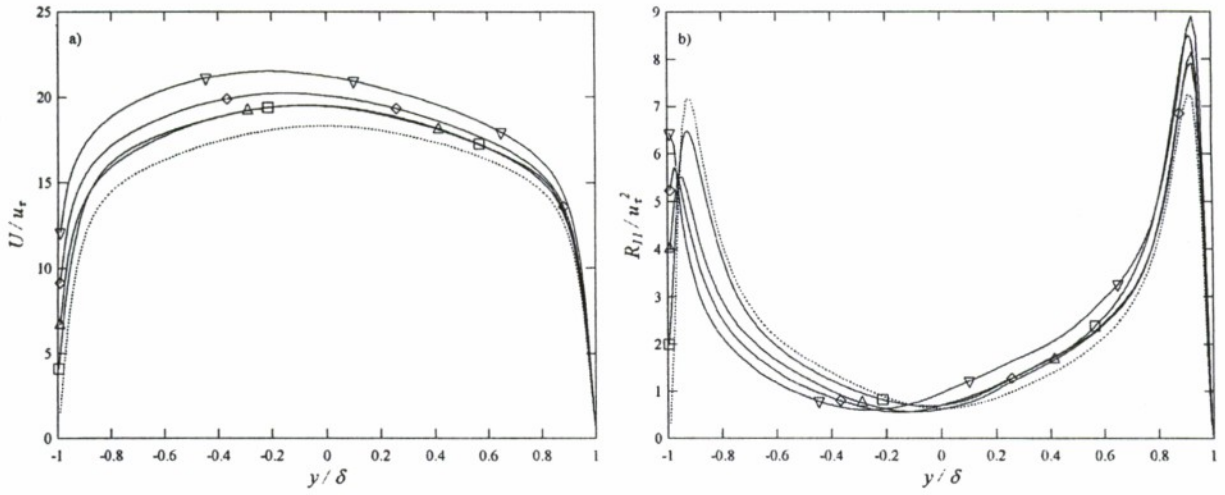

Figure 10 Velocity profiles (a) and Reynolds stress profiles (b) predicted from DNS of channel flow at a friction Reynolds number of $Re_\tau = 180$ over superhydrophobic surfaces with microridges having width-spacing of $15\mu m - 15\mu m$ (□), $30\mu m - 30\mu m$(Δ), $30\mu m - 50\mu m$(◊), and $30\mu m - 90\mu m$(∇). Additionally, smooth channel flow is shown for reference (...). The symbols are employed to differentiate lines, and do not reflect actual data points.

expected that equivalent drag reduction performance will be accessible to much finer microfeature spacings at higher Reynolds numbers. With fine superhydrophobic surfaces, little drag reduction may be evident until the viscous sublayer shrinks significantly, well past transition. This result appears promising for possible commercial applications of this technology. This is because small feature spacing results in a more robust superhydrophobic surface capable of maintaining a coherent air-water interface at larger static pressures, while at the same time ships that might benefit from such surfaces operate at Reynolds numbers significantly greater than those interrogated in the present experiments.

Numerical Simulations

The DNS code has now been extensively validated for turbulent flows against the benchmark simulations of Kim, Moin and Moser [35] for grid resolutions of 128^3 , 256^3 and 512^3 having Re_τ = 180, 395 and 590 respectively. The quantitative agreement between our code and the benchmark simulations gave us the confidence to simulate ultrahydrophobic surfaces having various arrangements of microridges and microposts at a number of different Reynolds numbers. As one example of the results from our DNS simulations, Figure 10ontains the average velocity profile and turbulent Reynolds stress profiles for an ultrahydrophobic surface containing a series of microridge geometries. The simulations predict a large slip velocity along the ultrahydrophobic wall, $u_{slip}/u_{mean} > 75\%$, and a shifting of the velocity towards the ultrahydrophobic wall. Additionally, the Reynolds stresses show a reduction in the Reynolds stresses near the ultrahydrophobic wall, $\Delta\tau > 35\%$, and a non-zero R_{11} and R_{33} due to the slip velocity in both the flow and vorticity direction along the ultrahydrophobic wall. In Figure 11, the slip velocity and shear stress reduction is compiled for all of the simulations performed to date at Re_τ = 180. The trends clearly show an increased effectiveness with increased microridge or micropost spacing. Additionally, the simulations show that for a fixed spacing that microposts outperform microridges, however, if we compare the two on the basis of percentage of shear-free air-water interface, then the microridges are more effective. In our most recent simulations, we found that that unlike in laminar flows, in turbulent flows, increasing the flow rate and Reynolds number results in an increase in the superhydrophobic drag reduction and slip velocity, although the slip length appears to go through a maximum before decreasing with increasing Reynolds number at high Reynolds numbers.

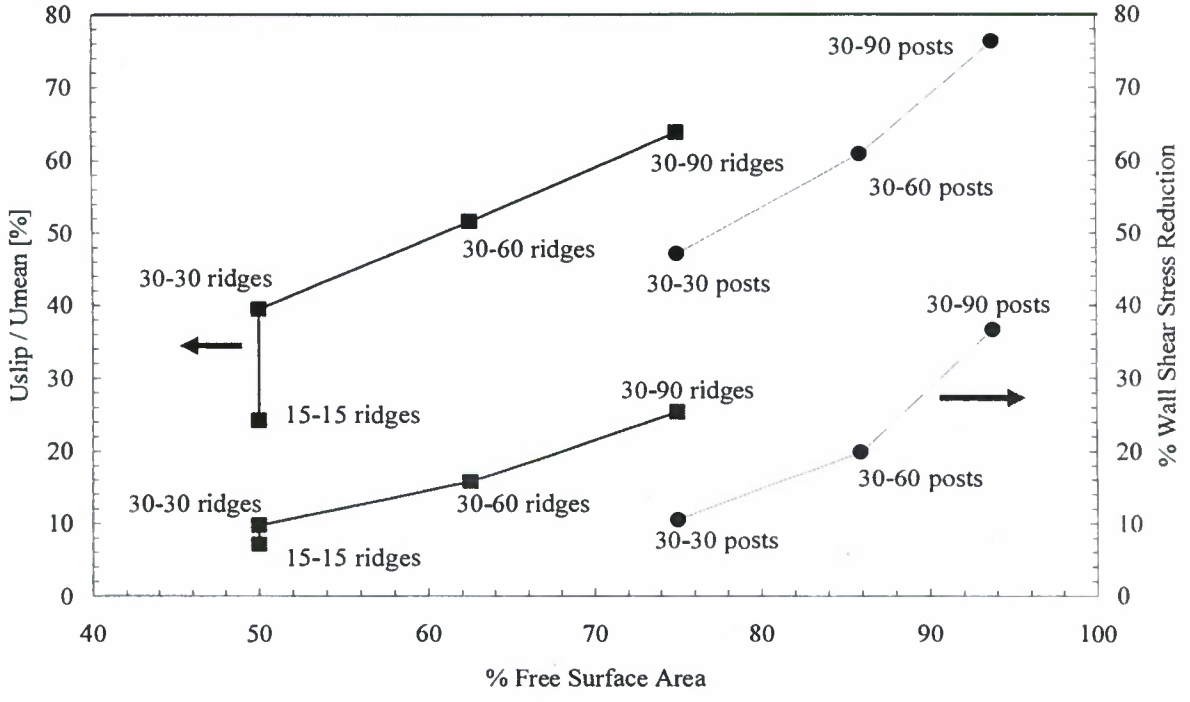

Figure 10. Slip velocity and shear stress reduction for a series of different ultrahydrophobic surfaces at a Reynolds number of $Re_\tau = 180$

References

[1] Barthlott, W., and Neinhuis, C., "Purity of the sacred lotus, or escape from contamination in biological surfaces," Planta, **202** (1997) 1-8.

[2] Ou, J., Perot, J. B., and Rothstein, J. P., "Laminar drag reduction in microchannels using ultrahydrophobic surfaces," Phys. Fluids, **16** (2004) 4635-4660.

[3] Ou, J., and Rothstein, J. P., "Direct velocity measurements of the flow past drag-reducing ultrahydrophobic surfaces," Phys. Fluids, **17** (2005) 103606.

[4] Ou, J., Moss, G. R., and Rothstein, J. P., "Enhanced mixing in laminar flows using ultrahydrophobic surfaces," Phys. Rev. E, **76** (2007) 016304.

[5] Watanabe, K., Yanuar, Katsutoshi, O., and Mizunuma, H., "Drag-reduction in flow through square and rectangular ducts with highly water repellent walls," Proceedings of the 2nd ASME Fluids Engineering Conference, (1996).

[6] Watanabe, K., Yanuar, and Udagawa, H., "Drag reduction of Newtonian fluid in a circular pipe with highly water-repellent wall," J. Fluid Mech., **381** (1999) 225-238.

[7] Jun, T., and Qunji, X., "Plate drag-reduction with low surface-energy coating in a water tunnel," Chinese Science Bulletin, **42** (1997) 307-310.

[8] Hsu, T.-R., *MEMS & Microsystems: Design and Manufacture*, McGraw-Hill, Boston, MA, 2002.

[9] McDonald, J. C., Duffy, D. C., Anderson, J. R., Chiu, D. T., Wu, H., Schueller, O. J. A., and Whitesides, G. M., "Fabrication of microfluidic systems in poly(dimethylsiloxane)," Electrophoresis, **21** (2000) 27-40.

[10] MacDonald, M. J., and Muller, S. J., "Shear rheology of polymer solutions near the critical condition for elastic instability," Rheol. Acta, **36** (1997) 97-109.

[11] Oner, D., and McCarthy, T. J., "Ultrahydrophobic surfaces: Effects of topography length scales on wettability," Langmuir, **16** (2000) 7777-7782.

[12] Perot, J. B., "Conservation properties of unstructured staggered mesh schemes," J. Comp. Phys., **159** (2000) 58-89.
[13] Perot, J. B., and Nallapatti, R., "Numerical Simulation of Free-Surface Flows Using a Moving Unstructured Staggered Mesh Method," ASME Fluid Engineering Summer Conference, Boston, MA (2000).
[14] Harlow, F. H., and Welch, J. E., "Numerical calculation of time dependent viscous incompressible flow of fluid with free surface," Phys. Fluids, **13** (1965) 1450.
[15] Chang, W., Giraldo, F., and Perot, J. B., "Analysis of an Exact Fractional Step Method," J. Comp. Phys., **180** (2002) 183-199.
[16] Perot, J. B., and Gadebusch, J., "A self-adapting turbulence model for flow simulation at any mesh resolution," submitted to Phys. Fluids, (2007).
[17] Perot, J. B., and Ramanathpura, M., "Performance of a Potential Flow Solver Using PC Clusters," ASME Fluid Engineering Summer Conference, Boston, MA (2000).
[18] Martell, M. B., Perot, J. B., and Rothstein, J. P., "Direct numerical simulations of turbulent flows over superhydrophobic surfaces," J. Fluid Mech., **620** (2009) 31-41.
[19] Martell, M. B., Rothstein, J. P., and Perot, J. B., "The effect of Reynolds number on turbulent flows over superhydrophobic surfaces," Submitted to Phys. Fluids, (2009).
[20] Daniello, R., Waterhouse, N. E., and Rothstein, J. P., "Turbulent drag reduction using superhydrophobic surfaces," In Press in Phys. Fluids, (2009).
[21] Daniello, R., Gabour, J., and Rothstein, J. P., "The effect of superhydrophobic surface geometry on turbulent drag reduction," Submitted to J. Fluid Mech., (2009).
[22] Rothstein, J. P., "Slip on Superhydrophobic Surfaces," in press in Annu. Rev. Fluid Mech., **42** (2010).
[23] White, F., M., *Viscous Fluid Flow*, McGraw-Hill, Boston, 2006.
[24] Spalding, D., B., "A Single Formula for the "Law of the Wall"," ASME Journal of Applied Mechanics, **Series E** (1961) 455-458.
[25] Martell, M., B., *Simulation of Turbulence Over Superhydrophobic Surfaces*, Master of Science Thesis, University of Massachusetts, 2008.
[26] Ybert, C., Barentin, C., Cottin-Bizonne, C., Joseph, P., and Bocquet, L., "Achieving large slip with superhydrophobic surfaces: Scaling laws for generic geometries," Physics of Fluids, **v 19** (2007) p 123601.
[27] Moody, L., F., "Friction Factors for Pipe Flow," American Society of Mechanical Engineers -- Transactions, **66** (1944) 671-678.
[28] Martell, M., B., Rothstein, J., P., and Perot, J., B., "Direct Numerical Simulation of Turbulent Flow over Ultrahydrophobic Surfaces," J. Fluid Mech., (2008).
[29] Min, T., and Kim, J., "Effects of hydrophobic surface on skin-friction drag," Physics of Fluids, **16** (2004) L55 -L58
[30] Fukagata, K., Kasagi, N., and Koumoutsakos, P., "A theoretical prediction of friction drag reduction in turbulent flow by superhydrophobic surfaces," Physics of Fluids, **18** (2006) 051703 - 051703
[31] Philip, J. R., "Flows satisfying mixed no-slip and no-shear conditions," Z. Angew. Math. Phys., **23** (1972) 353-372.
[32] Philip, J. R., "Integral properties of flows satisfying mixed no-slip and no-shear conditions," Z. Angew. Math. Phys., **23** (1972) 960-968.
[33] Ou, J., and Rothstein, J. P., "Direct velocity measurements of the flow past drag-reducing ultrahydrophobic surfaces," Physics of Fluids, **17** (2005) -.
[34] White, F. M., *Viscous Fluid Flow*, McGraw-Hill, New York, 1991.
[35] Kim, J., Moin, P., and Moser, R., "Turbulence statistics in fully developed channel flow at low Reynolds number," J. Fluid Mech., **177** (1987) 133-166.